ELECTRICAL CONDUCTIVITY OF CALCIUM FLUORIDE POWDER COMPACTS

A Thesis Submitted
In Partial Fulfilment of the Requirements
for the Degree of
MASTER OF TECHNOLOGY

BY
RAM SHRESHTHA SHARMA

to the

DEPARTMENT OF METALLURGICAL ENGINEERING
INDIAN INSTITUTE OF TECHNOLOGY KANPUR
OCTOBER 1972

CERTIFICATE

Certified that this work on 'Electrical Conductivity of Calcium Fluoride Powder Compacts', has been carried out under my supervision and that it has not been submitted elsewhere for a degree.

(Hem Shanker Ray)
Assistant Professor
Department of Metallurgical Engg.
Indian Institute of Technology
Kanpur

ACKNOWLEDGEMENTS

I have a great pleasure in recording my sincere gratitude to Dr. H.S. Ray for his valuable guidance and encouragement throughout this work.

I also thank Dr. G.N.K. Iyengar of I.I.Sc. Bangalore for his keen interest in this work.

I am very thankful to Dr. D. Chakraborty for the valuable discussions which I had with him from time to time.

I wish to thank Mr. Chandon Roy who collaborated in this work as Govt. of India trainee. I also thank Mr. S. Basu, Dr. K.P. Jaganathan, Mr. S. Mazumdar, Mr. C.B. Choudhary, Mr. K.L. Luthra, Mr. A. Ali, Mr. S.P. Bhat, Mr. K.P.S. Verma and my other friends who helped me during the work.

Last but not least, I thank Shri B. Sharma, Shri R.K. Prasad of Ceramics Lab. and Shri K.P.Mukherjee of Physical Met. Lab. for helping me even out of the way during the experimental work.

R.S. Sharma

CONTENTS

LIST OF FIGURES

LIST OF TABLES

SYNOPSIS

Electrical conductivities of CaF_2 powder compacts, prepared under various compacting pressures, have been studied at various temperatures. All samples were prepared from the same powder thus eliminating possible effects of particle size.

At all temperatures conductivity is higher than that of CaF_2 single crystal for which reliable data are available in the literature. Higher values are attributed to enhanced conduction along grain boundaries which form a continuous matrix in polycrystalline material. Samples prepared under higher compacting pressures show higher values of conductivity due to the presence of more extended grain boundary regions.

The polycrystalline material may be used in various physicochemical measurements where a fluorine ion conducting solid electrolyte is required. It would be attractive specially for liquid systems as crucible may be fabricated easily from powder compacts.

CHAPTER I

INTRODUCTION

Solid electrolytes, in general, are solid substances which show predominant ionic conduction due to the existance and mobility of point defects in their crystal lattice in a considerable range of temperature and partial pressure. Electrochemical techniques using solid electrolytes have been used widely in the determination of thermodynamic and kinetic data pertaining to systems of metallurgical interest. The advantage of this technique began to be realized after Kiukkola and Wagner[1] had demonstrated that ZrO_2 stablized with 15% CaO, was a purely ionic conductor at oxygen pressures between 1 and 10^{-20} atm at 850°C. Their classic work on ZrO_2 - CaO and other solid electrolytes paved the path for the further development of solid electrolytes.

The renewed interest in the solid electrolytes[2] has concided with the improvement in certain solid electrolytes and the achievement of a better understanding of the mechanism of transport in these solid ionic materials.

CaF_2 which has fluorite structure is an important solid electrolyte among fluorides. The extensive investigation by Ure[3] on CaF_2 proved that it is an ionic conductor and fluorine ion F^- is responsible for conductance. His investigation was connected with pure and doped single crystals.

Many workers have used this material for determination of free-energies of formation of fluorides, carbides, phosphides and other systems.

Aim of the Present Work:

The aim of present investigation is to study the electrical conductivity of CaF_2 in powder compact form. It is well known that growing a single crystal is a troublesome job and at the same time it is a costly affair. Besides a single crystal would normally be a pellet. On the other hand, powder compacts may be made in crucible form. Crucibles may be used in investigations on liquid systems.

The main aim of the investigation was to study the electrical conductivity of CaF_2 powder compacts made under different conditions, as a function of temperature. The values are to be compared with those for single crystals.

CHAPTER II

CaF_2 AS SOLID ELECTROLYTE

A solid electrolyte as the name implies, is a stable solid phase which conducts electricity ionically. The material allows one or more kinds of ions to migrate through its lattice when a tendency for migration exists. This tendency is induced by a potential gradient generated either through an applied voltage or through a chemical potential gradient of the migrating ion(s).

In general most solid electrolytes conduct both ionically as well as electronically. However, under certain ranges of temperature and chemical potentials of the migrating species, many solid electrolytes exhibit predominant ionic conduction. These electrolytes, of course, can be employed in electrolytic cells only when the electronic conduction is negligible.

Common solid electrolytes are of three kinds, namely, halides, simple oxides and oxide solid solution. A complete list of known solid electrolytes is given in the Table 2.1.

2.2 Fluorite Structure:

Materials[5] with fluorite structure of which CaF_2 is the prototype are an important class of materials which includes the alkaline earth fluorides and such important oxides as UO_2, ThO_2 and PuO_2. These oxides are important

Table 2.1

List of known Solid Electrolytes

Ion exhibiting predominant conduction	Compound
Fluorine (F^-)	CaF_2, MgF_2, PbF_2, NaF, BaF_2, SrF_2
Chlorine (Cl^-)	$BaCl_2$, $PbCl_2$, $SrCl_2$
Bromine (Br^-)	$BaBr_2$, $PbBr_2$, NaBr $\lvert Na^+, Br^- \rvert$, KBr $\lvert K^+, Br^- \rvert$
Iodine (I^-)	PbI_2, (Pb^{2+}, I^-), KI (K^+, I^-)
Silver (Ag^+)	AgI, AgCl, AgBr, Ag_3SBr, Ag_3SI, Ag_2HgI_4, KAg_4I_5, $PbAg_4I_5$, $NH_4Ag_4I_5$
Copper (Cu^+)	CuI, CuCl, CuBr
Magnesium (Mg^{2+})	MgO
Oxygen (O^{2-})	$Zr_{1-x}M_x^{2+}O_{2-x}$, $Zr_{1-x}M_2^{3+}O_{2-(x/2)}$ $Th_{1-x}M_x^{3+}O_{2-(x/2)}$, $Th_{1-x}M_x^{3+}O_{2-(x/2)}$
Aluminium (Al^{3+})	Al_2O_3
Sodium (Na^+)	NaF (Na^+, F^-), NaCl (Na^+, Cl^-) NaBr (Na^+, Br^-), $Na_2O.\ 11Al_2O_3$
Potassium (K^+)	KCl (K^+, Cl^-), KBr (K^+, Br^-) KI(K^+, I^-), $3K_2O.0.2\ Li_2O.10Al_2O_3$
Alkali metal ions (Na^+ and K^+)	SiO_2 (quartz) $3\ Al_2O_3.2SiO_2$ (Mullite[e])
Lithium (Li^+)	LiH

nuclear materials. The cubic stabilized forms of ZrO_2 and HfO_2 and C modifications of the rare earth sesquioxides are derivatives of this basic structure.

A coordination of 8:4 is found in the CaF_2. Here the calcium ions are arranged at the corners and face centers of a cubic unit cell and the fluorine ions are at the centers of the eight cubelets into which the cell may be divided. The unit cell[6] of the cubic structure of fluorite, calcium fluoride is shown in the Figure 2.1. Each calcium ion is therefore coordinated by eight fluorine neighbours at the corners of a cube while the calcium neighbours of a fluorine ion are four in number, disposed at the corners of a regular tetrahedron.

~~Materials crystallizing in the fluorite structure are unusual among ceramics because of the diffusion of anions is far more rapid than that of cations.~~ These materials normally show anion electrolytic behaviour over wide nonmetals partial pressure range. Matzke[7] suggested that CaF_2 should be a good model for UO_2 and ThO_2 on the basis of the similarity in structure and lattice parameters. Similar arguments might be applied to the stabilized forms of ZrO_2 and HfO_2 and to the C-type rare-earth oxides.

2.3 Conduction in Fluorides:

It is known that a number of metallic halides, those of the alkali and alkaline earth metals in particular, are total ionic conductors. But for many high temperatures thermodynamic studies only fluorides are suitable on account of their high melting points.

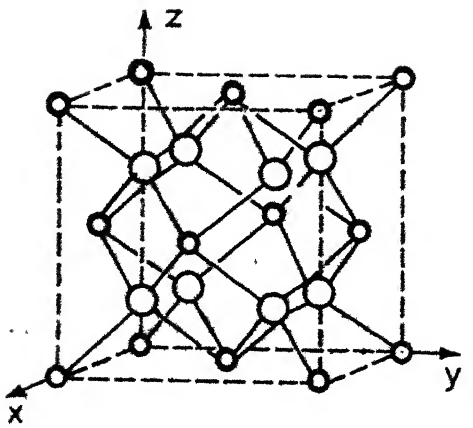

●:Ca O:F

FIG. 2.1 CLINOGRAPHIC PROJECTION OF THE UNIT CELL OF THE CUBIC STRUCTURE OF FLURITE CALCIUM FLUORIDE

Alkali and alkaline earth fluorides are stoichiometric. Due to the wide energy gap between the valence and conduction bands, the contribution of electronic conduction could be negligible. Hence only intrinsic ionic defects due to the thermal disorder can be envisaged in these fluorides. Taking into account the maintenance of electrical charge neutrality, four possible types of defects can occur in these crystals. They can be mentioned as:

(i) Frenkel disorder involving equal number of positive ion vacancies and interstitial positive ions.

(ii) Anti-Frenkel disorder with equal concentrations of negative ion vacancies and interstitials.

(iii) Schottky disorder with equal concentrations of positive and negative ion vacancies and, in the same ratio as that in the crysl

(iv) Anti-Schottky disorder type with equal positive and negative interstials.

A simple representation of main types of lattice disorder is shown in Figure 2.2 schematically in two dimensions for alkali-halides.

Even though more than one type of disorder can occur, the one with the lowest activation energy predominates. The anti-Frenkel and the anti-Schottky types are less frequently encountered in ionic crystals. It is highly essential that the defect chemistry of the fluorides is fully understood before incorporating them as solid electrolytes in the solid state galvanic cells.

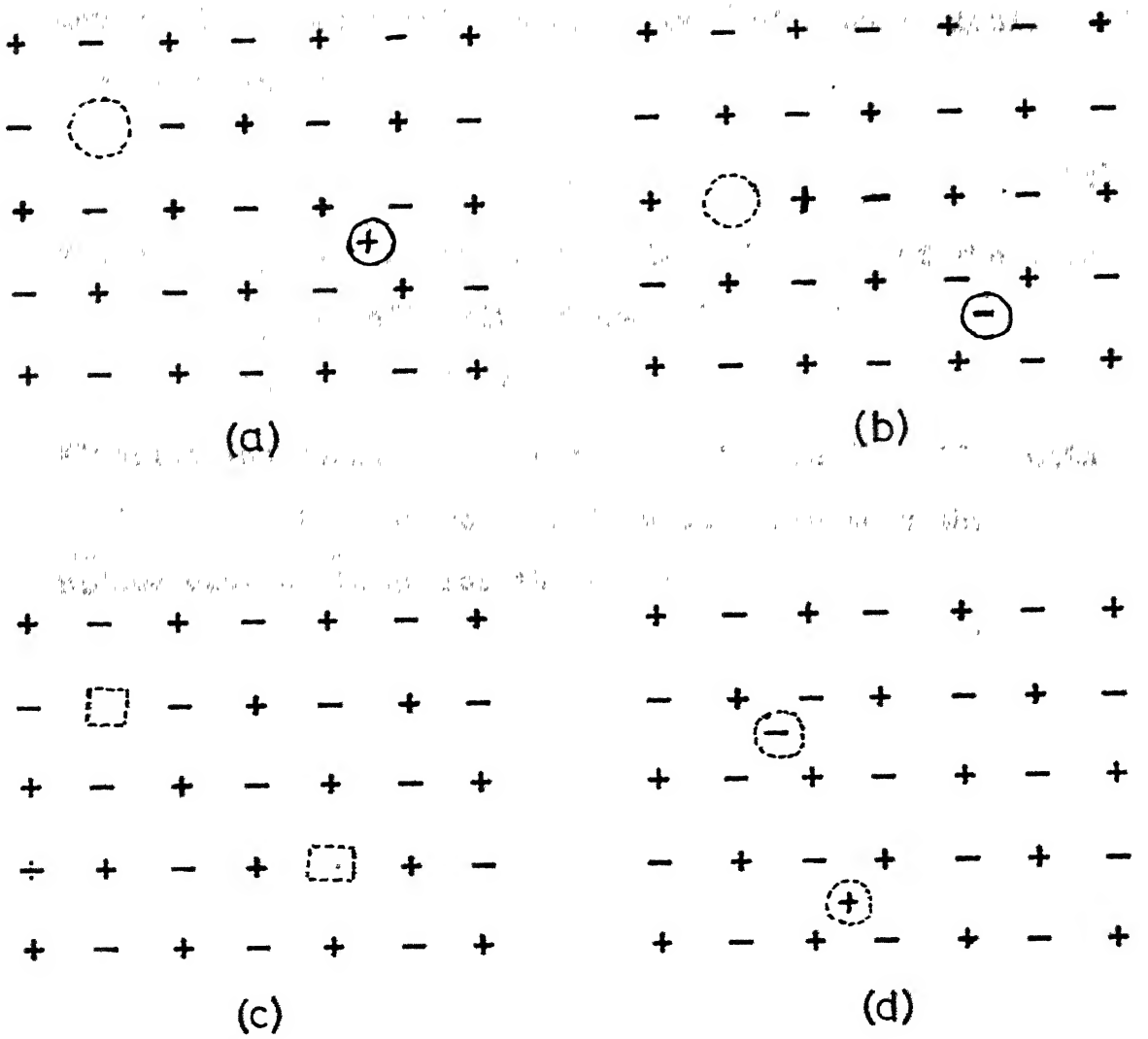

FIG. 2.2 MAIN TYPES OF LATTICE DISORDER PRESENTED SCHEMATICALLY IN TWO DIMENSIONS FOR ALKALI HALIDES.

(a) Frenkel disorder

(b) Anti-Frenkel disorder

(c) Schottky disorder

(d) Anti-Schottky disorder

The details of the defect structure and the ionic charge transport are mainly derived from conductivity measurements. The electrical conductivity σ of a solid ionic conductor is given by,

$$\sigma = \Sigma_k e_k n_k u_k \qquad (1)$$

where n_k = the density of imperfections of the k-th type.

e_k = effective charge of imperfection.

u_k = mobility.

Fluoride ion conduction can be expected in fluorides with anti-Frenkel type defects. This would mean that the cationic ~~radius~~ mobility must be ~~large~~ small for the given crystal arrangement. Conductivity measurements are normally carried out with pure as well as doped crystals.

2.4 Conductivity of Doped and Pure CaF_2:

The suitability of a material as a solid electrolyte requires that it should be a total ionic conductor, even a small contribution of the electronic conductivity will tend to large errors. Electronic conductance will tend to lower the theoretical e.m.f. in galvanic cell according to the relation[8]

$$E_{(observed)} = E_{Theoretical} \left((1 - t_e) \right.$$

where t_e = electronic transport number.

In case of CaF_2 the neutral calcium and fluorine atoms have the electronic configuration as,

$$Ca = 1S^2\ 2S^2\ 2p^6\ 3S^2\ 3p^6\ 4S^2 \text{ and}$$

$$F = 1S^2\ 2S^2\ 2p^5.$$

In ionic form the configuration changes to,

Ca^{2+} = $1S^2\ 2S^2\ 2p^6\ 3S^2\ 3p^6$ (Argon configuration)

F^- = $1S^2\ 2S^2\ 2p^6$ (Ne-configuration).

Both ions posses stable inert gas electronic configurations which implies a very small intrinsic electronic disorder and a correspondingly low value for the electronic conductivity.

Ure[3] has studied the conductivity and diffusion processes in single crystal (pure and doped) in detail and concluded that major disorder present in CaF_2 is the anti-Frenkel type i.e. F^- vacancies and interstials. His conclusion is based on the results of three transference number experiments. His results are:

(i) the F^- transference number in NaF doped CaF_2 is unity and the conductivity increase on adding NaF is very large. The large conductivity increase shows that the imperfections which are introduced by doping control the conductivity; and the large F^- transference number proves that these imperfections are F^- vacancies rather than Ca^{++} interstials.

(ii) Zintl and Udgard showed by means of density and X-Ray lattice constant measurements that YF_3 added to CaF_2 introduces F^- interstials. This is confirmed by the fact that the conductivity increase on adding YF_3 is appreciable and that the F^- transference number of the YF_3- doped crystal is one.

(iii) The Ca^{++} transference number in pure CaF_2 is 10^{-6} at 1000°C. If the Schottky or anti-Schottky disorder type were present, the Ca^{++} transference number would be,

$$t_{Ca} = \frac{U_{Ca}}{U_{Ca} + U_F} \qquad (2)$$

where U_{Ca} = the mobility of the Ca^{++} imperfection.

U_F = the mobility of the F^- imperfection.

In other ionic crystals the corresponding mobility ratio is of the order of 10^{-1} to 10^{-3} at temperatures within four or five hundred degrees of the melting point. It seems improbable that it would be as small as 10^{-6} here as would be required if the Schottky or anti-Schottky disorder type were predominant, the Ca^{++} transference number would be close to one.

The main conclusion of Ure[3] is that Anti-Frenkel type of disorder exists in CaF_2 and that the transport-number of the fluoride ion, t_{F^-}, is almost unity in the temperature range 690° - 920°C.

Short and Roy[9] studied the defect character in calcium fluoride - Yttrium Fluoride crystalline solutions and confirmed that interstitial F^- is the predominant defect in crystalline solutionsof YF_3 in CaF_2.

Barris and Taylor[10] have studied the lattice disorder in some CaF_2 type crystals like BaF_2 and SrF_2 and by measuring ionic conductivity with single crystals (pure and doped with monovalent and trivalent cations) they have shown a consistent trend in the scopes of $\log\sigma$ vs $\frac{1}{T}$ plot of the conductivity data. They have shown by the analysis of conductivity isotherms that an anion Frenkel thermal disorder model for the fluorides exists.

2.5 Examples of CaF_2 Used as Solid Electrolyte:

CaF_2 has been used for the determination of free-energy of formation of several metal fluorides and for other than fluorides. Markin[11] has summerized the Galvanic cells reversible to fluoride ions.

Lofgren and McIver[12] and Egan and Heus have measured the Free-energy of formation of several metal fluorides. Markin and coworkers[13] and Lofgren and McIver measured the e.m.f. of the following cells:

Cell			e.m.f. (V) at 600°C
Ni,NiF_2	CaF_2	Al,AlF_3	1.720 ± 0.003
Ni,NiF_2	CaF_2	Mg,MgF_2	2.343 ± 0.003
Ni,NiF_2	CaF_2	Fe,FeF_2	0.374 ± 0.003
Al,AlF_3	CaF_2	U,UF_2	0.078 ± 0.003
UF_3,UF_4	CaF_2	Al,AlF_3	0.821 ± 0.004
UF_3,UF_4	CaF_2	Mg,MgF_2	1.437 ± 0.003
Ni,NiF_2	CaF_2	UF_3,UF_4	0.905 ± 0.004
UF_3,UF_4	CaF_2	U,UF_3	0.899 ± 0.002

Egan and Heus[14] have measured the e.m.f. of following cell using CaF_2

Cell			e.m.f. (V) at 600°C
Mg,MgF_2	CaF_2	Th,ThF_4	-0.310 ± 0.005
Th,ThF_4	CaF_2	Al,AlF_3	-0.310 + 0.003
U,UF_3	CaF_2	Al,AlF_3	-0.070 ± 0.003
Th,ThF_4	CaF_2	Ni,NiF_2	-1.980 ± 0.005

As it has been mentioned earlier that CaF_2 has been used for determination of free-energy of formation of compounds

other than fluorides. In this category comes oxides and related compounds, carbides, borides, sulphides, phosphides. Tables 2.2 and 2.3 show its application for oxides and related compounds and for other trans fluorides and oxides.

Table 2.2

Application of the galvanic cells in the measurement of the free energy of formation of oxides and related compounds

System	Compounds	Ref.
Ca-O	CaO	15
Mg-O	MgO	
Zn-O	ZnO	
Al-O	Al_2O_3	
Ca-Si-O	$CaO-SiO_2$	16
	$3CaO-2SiO_2$	
	$2CaO-SiO_2$	
Ca-Ti-O	$CaO-TiO_2$	17
	$4CaO-TiO_2$	
Ca-W-O	$CaWO_4$	18
Ca-Fe-O	$CaO-Fe_2O_3$	19
	$2CaO-Fe_2O_3$	
Ca-Cr-O	$CaCrO_4$	20
Ca-V-O	$3CaO-V_2O_5$	21
	$2CaO-V_2O_5$	
	$CaO-V_2O_5$	
Ca-B-O	$3CaO-B_2O_3$	
	$2CaO-B_2O_3$	
	4	

Table 2.3

Application of CaF_2 galvanic cells in the measurement of the free-energy of formation of compounds other than fluorides and oxides

System	Compound	Ref.
Th-S	ThS	22
	Th_2S_3	
	Th_7S_{12}	
Th-P	$ThP_{0.55-0.96}$	23
Th-C	$ThC_{1-x(x=0.04-0.34)}$	24
	ThC_2	25
	ThC	
U-C	UC_2	26
	UC_3	
Th-B	ThB_4	27
	ThB_6	
Mn-C	Mn_7C_3	28
	Mn_5C_2	
	$Mn_{23}C_5$	

CHAPTER III

EXPERIMENTAL PROCEDURE

3.1 Sample Preparation:

CaF_2 powder of 99.94% purity was taken as supplied under the name certified calcium fluoride by Fisher Scientific Company, U.S.A. The analysis of the powder is given in the Table 3.1. Powder weighing approximately 2 gm. was pressed in the form of cylindrical pellets in a 1/2 inch die at different pressures 5000 lbs. 7000 lbs, 11000 lbs, 13000 lbs and 15000 lbs. in Carver Laboratory Press (Hydraulic). The pellets were sintered in inert atmosphere. Nitrogen gas was passed through calcium chloride tower to remove any moisture and then it was passed through a copper-turning furnace to remove oxygen. The sintering was done at 950°C for 4 hrs.

These sintered pellets were painted on top and bottom faces with Engel hard No. 6926 unfluxed platinum paint. The thinning of the paste was done with tempentine oil. The painted samples were fired at 850°C for nearly 3 to 4 hrs. After the firing the resistance between different points on the painted faces were measured and it was made sure that the resistance was below half ohm. In some cases the resistance was more than 1 ohm. In those cases the pallets were again painted and fired to show resistance less than half ohm.

TABLE 3.1

Analysis of Calcium Fluoride

Formula: CaF_2

Formula weight = 78.08

Constituents	Weight in percent
Chloride (Cl)	0.01
Heavy metals (as Pb)	0.003
Ammonia (NH_3)	0.01
Sulphate (SO_4)	0.03
Iron (Fe)	0.001
Barium (Ba)	0.005

3.2 Apparatus:

The apparatus consisted of three main parts: (i) Furnace, (ii) Cell Assembly and (iii) Gas Train. These are briefly described below:

(i) Furnace:

The furnace was a Nichrome Wire would 'tubeless' furnace.

A split wooden pattern was made and a winding was laid on it. Refractory cement was applied on the windings and the assembly was introduced in a brick work. It was then dried. After drying of cement the wooden pattern was withdrawn. The brick structure was insulated using magnesia powder.

Temperatures in the furnace were controlled by a Pt-Pt-Rh thermocouple placed in between the winding and Inconel tube in which the cell assembly was placed.

(ii) Cell Assembly:

The cell assembly with the furnace is shown in the Figure 3.1. The sample holder is placed in the inconel tube. There is provision in the inconel tube from the bottom for the entrance of purified argon gas which ultimately leaves the cell assembly through a gas outlet. The gas outlet is connected with a rubber tubing to a bubbler for the exit of the argon gas. The cell assembly consists of a chromel-alumel thermocouple for measuring the temperature inside the cell assembly.

There is a central tube of stainless steel through which the two Platinum Wires welded to the discs pass which form the electrodes.

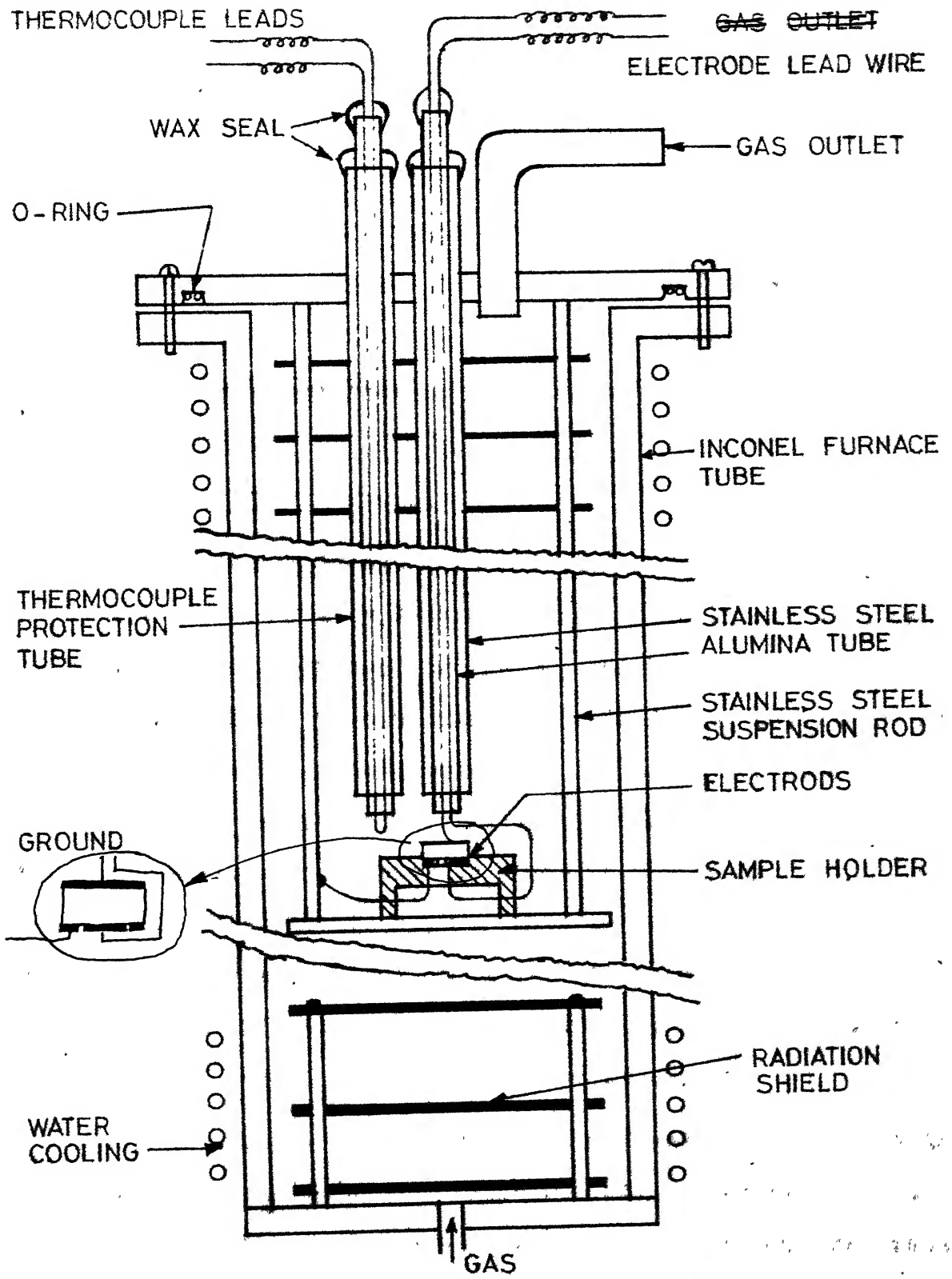

FIG. 3.1 DIAGRAMMATIC SKETCH OF THE CELL ASSE ASSEMBLY WITH FURNACE

(iii) Gas-Train:

For circulating purified argon gas in the cell assembly a gas-train was constructed. It consists of glass-towers containing $CaCl_2$(anhydrous) for absorbing moisture in the gas. There is a copper gauge furnace to remove any oxygen from the gas and finally the gas passes through a Titanium powder furnace to further purify the gas. From Titanium furnace gas comes to chamber from where it goes to the inconal tube through a rubber tubing.

3.3 Conductivity Measurement:

Conductivity was measured with an Impedence Bridge of type 1608 - A made by General Radio. This bridge is a self-contained impedance-measuring system, which included six bridges for the measurement of capacitance, conductance, resistance and inductance as well as the generators and detectors necessary for dc and 1-KC ac measurements. The bridge circuit which was used for conductivity measurement is shown in the Figure 3.2. The basic bridge accuracy is 0.1%. This is a function of the accuracy of the adjustment and stability of the bridge arms. The instrument is initially calibrated to an accuracy of $\pm$ 0.05% or better and should hold the 0.1% accuracy.

The sample was placed on ar refractory sample holder between thin platinum discs. Platinum electrodes extensions were connected to the Impedence bridge. The temperatures were recorded with the chromel-Alumel thermocouple placed just near the sample using a LN Potentiometer. By suitably choosing the scale the conductivity was measured.

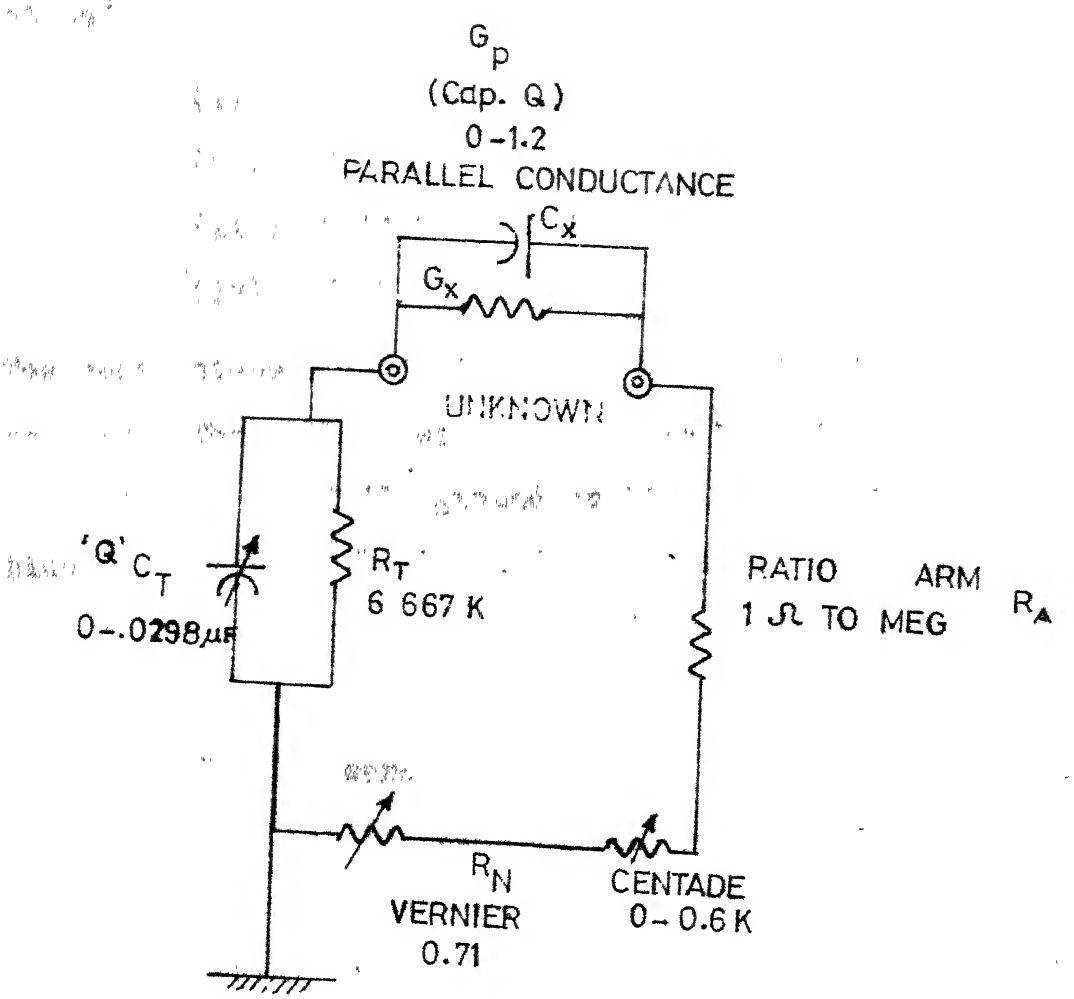

FIG. 3.2 IMPEDENCE BRIDGE CIRCUIT EOR MEASURING CONDUCTIVITY

3.4 Sample Preparation for Microstructure Study:

Calcium Fluoride is a ceramic material and for any ceramic material the general procedure for preparation of samples for microstructure study consists of the following steps[30].

(i) Mounting

(ii) Grinding

(iii) Polishing and

(iv) Etching.

The above steps were followed for sintered calcium fluoride pellets. The pellets were mounted in bakelite mounts. Mounted samples were carefully ground on 240-, 320- grit silicon carbide dry papers on belt grinding machine. To minimize surface damage the 320 - grit grind should be prolonged using diminishing pressures.

Samples were polished on 400- and 600- grit emery paper. After that the samples were polished on 4/0, 2/0, 4/0 emery papers one by one and removing the scretches from previous one on polishing wheel. Final polishing was done with cerium oxide on polishing wheel on micro cloth.

A number of etchants were tried to reveal the microstructure of the polished specimens and finally 10% H_2SO_4 boiling was found suitable for the purpose. The etching time was kept as 1 to 1.5 minutes in boiling condition.

3.5 Microstructure Study:

The etched samples were viewed under Metallurgical microscope (optical) and the microstructure obtained was photographed by camera.

The film was illuminated under Microform Reader. The magnification was 19.56 X. A length of 30 cm was marked on a plain paper and the grains were counted in that length. The measurements was done along random sections usually horizontally, vertically and diagonally from both ends of the film. The number of grains for all the samples were counted in this manner.

Grain size was obtained from counting the grains under the microscope.

RESULTS AND DISCUSSIONS

4.1 Densification:

The CaF_2 powder was compacted at different pressures ranging from 5000 lbs to 15000 lbs and then sintered at 950°C for 4 hours. The resulting green densities and sintered densities are given in the Table 4.1. From the table it was found that as compacting pressure increases both the green densities and sintered densities increase.

One of the most widely used methods of producing refractory shapes is that of cold pressing and sintering and in practice, the rate at which sintering occurs and the porosity of the final product are important. As it is known that for any component which can be prepared by pressure forming operation a porosity of 40 percent is tolerated.

In the present study the final porosity is lower at the higher pressures. This should be due to the lower initial porosity of the more highly pressed compacts. In otherwords, for producing a more dense sintered product a more dense green compact is necessary.

Samples were sintered at 950°C as suggested by Allison and Murray[31]. In their study of 'A fundamental investigation of the mechanism of Sintering' they used different temperatures and finally recommended 950°C. The sintering time they used

Table 4.1

Green densities and sintered densities of the pellets at 950°C for 4 hrs.

Theoretical density = 3.18 gm/cc

Sample	Pressure	Gree density gm/cc	% of Theoretical density	Sintered density gm/cc	% of Theoretical density
A	5000 lbs	1.8377	57.78	2.745	86.32
B	11000 lbs	1.981	62.29	2.76	86.79
C	13000 lbs	2.014	63.33	2.8	88.05
D	15000 lbs	2.067	65.00	2.89	90.88

was varied from 10 minutes to 3 hrs. In the present study the sintering time was kept 4 hours. for all samples. The densification obtained was nearly 91 percent of the theoretical density. The aim of the present study being make a crucible of CaF_2 which can be used for electrochemical study for liquid systems. Keeping in view this fact in mind it is necessary to have a product of higher densification. In case of liquids they may penetrate if the container is porous. For getting more dense product a slightly higher temperature should be tried.

Sintering mechanism has been studied by Allison and Murray. As regards the sintering behaviour the effect of particle size is also to be considered. The effect is partly reflected in the difference in the initial porosities of the compacts. With decreasing particle size, better packing is obtained resulting in a decreased initial porosity for the same compacting pressure. The sintered porosity is also lower. In the present work the effect of particle size has not been studied. Different samples were prepared from the same powder. The initial particle size remained uniform. The powder was below 100 - mesh and 70 percent was below 400 mesh.

4.2 Electrical Conductivity:

The variation of conductivity (σ) with respect to temperature is given by the well known equation,

$$\sigma = A \exp(-E/kT) \qquad (3)$$

where A is a pre-exponential term and E is the activation

energy for conduction which depends upon the actual mechanism regulating conductivity.

K is Boltzmanns constant and T is the absolute temperature. The value of E is estimated from the scope of the plot of $\log\sigma$ Vs. 1/T.

In general the $\log\sigma$ Vs. 1/T plot for is found to follow a general pattern as shown in the Figure 4.1a. Various conductivity data available in the literature conform to this general trend. As examples results on electrical conductivity measured by Graham[32] and others and on CaF_2 (pure and doped) by Ure may be cited. The plot indicates three distinct regions all characterized by different activation energies. In high temperature (intrinsic) region where the concentration of defects is high and its effect is more compared to the impurity concentration. The scope is given by

$$-(\tfrac{1}{2}\ H_f + H_m)/K$$

where,

H_f = Enthalpy of formation for defects

H_m = Enthalpy for the motion of defects

K = Boltzmanns constant.

In the lower temperature (extrinsic) region the slop corresponds to $-H_m/K$. At still lower temperatures, where association becomes dominant, the slope attains the value $-(\frac{1}{2}\ Ha + Hm)/K$ where Ha is the enthalpy for association of defects. Most often the various parts of the curve are not as well separated in practice as is shown in Figure 4.1a and

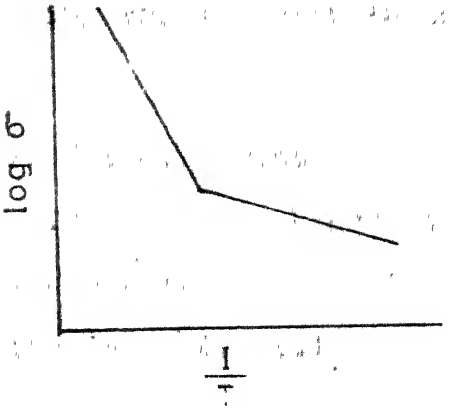

(a)

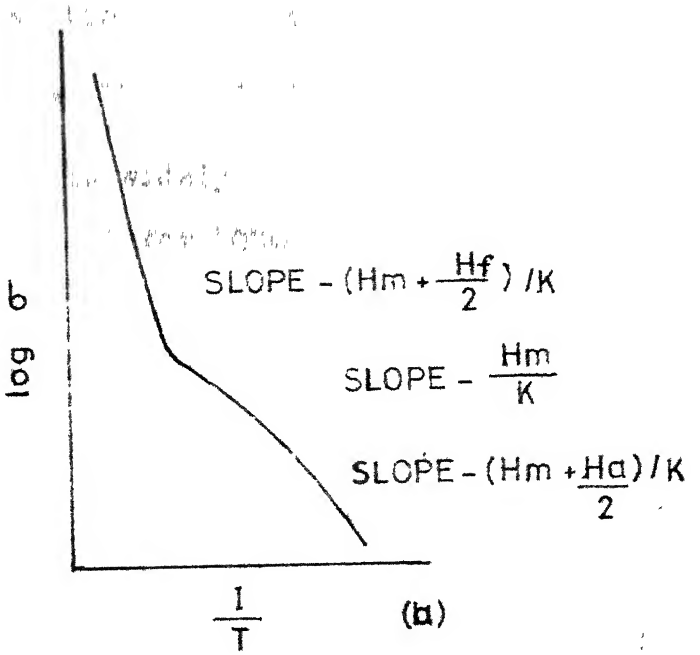

FIG. 4.1 (a) GENERAL SHAPE OF A CONDUCTIVITY VS $\frac{1}{T}$ PLOT

(b) IDEALISED SHAPE OF σ VS $\frac{1}{T}$ FOR ALKALI HALIDES

association range is not separated from the extrinsic region. The usual shape of a conductivity vs. 1/T plot is shown in Figure 4.1b.

The conductivity values for different temperatures and pressures are given in Table 4.2 (a to e). Figure 4.2 gives the variation $\log \sigma$ vs 1/T, where σ is conductivity in $(\text{ohm-cm})^{-1}$ and T is temperature in ^{o}K. All conductivity data presented here for sintered specimens have been normalized for porosity using the relation

$$\sigma_{\text{normal}} = \sigma_{\text{measured}} \frac{\rho_{\text{Theoretical}}}{\rho_{\text{Measured}}} \qquad (4)$$

where ρ_{measured} = the density of the sintered specimen,

$\rho_{\text{theoretical}}$ = Theoretical density.

This procedure is widely recommended[33] for correction due to porosity. The plot for 7000 lbs. compacting pressure has not been shown for the sake of clearity. However, it confirms to the general trend.

In one trial run for conductivity measurement data for heating and cooling did not match. The descrepancy, however, was eliminated on reheating. The initial heating values were smaller than the initial cooling, Values. This could be completely eliminated by preheating the sample to a temperature of approximately $1000^{o}C$. This was achieved simultaneously with the firing of platinum electrodes on the sample.

The initial hysteresis is presumably due to dimensional changes and due to the presense of defects in excess of the equilibrium concentration. Subsequent measurements were

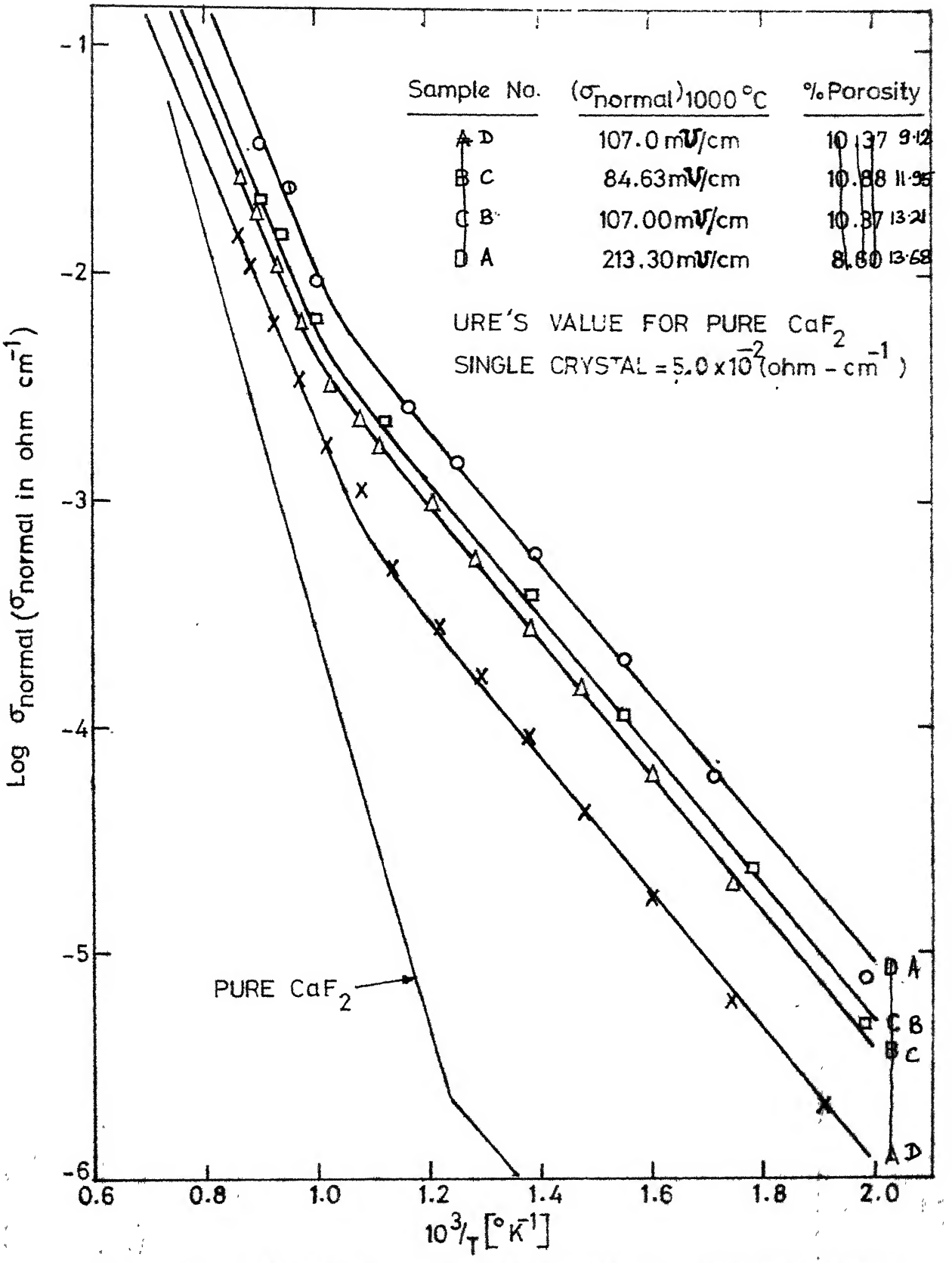

FIG. 4.2 ELECTRICAL CONDUCTIVITY VARIATION WITH TEMPERATURES FOR DIFFERENT COMPACTING PRESSURES

Table 4.2: A.C. conductivity at different temperatures for compacting pressure 5000 lbs.

6

History of the Sample	Temp. $T^{o}K$	$\frac{1}{T} \times 10^{3}$ $(K^{o})^{-1}$	Specific conductivity (ohm $^{-1}$ cm)$^{-1}$	Log σ	Log σ T	Remarks
Sample A	523	1.911461	2.08040×10^{-6}	-5.68186	-2.9628	
	573	1.74471	6.15854×10^{-6}	-5.21052	-2.4525	
Weight=1.951 gm	623	1.60472	17.07681×10^{-6}	-4.76769	-1.8735	
Length=0.736 gm	673	1.48553	41.13663×10^{-6}	-4.39368	-1.5578	
Dia =1.094 cm	723	1.38281	82.5783×10^{-6}	-4.08315	-1.2240	
Bottom electrode G.Ring Dia=0.893cm	773	1.29339	167.52717×10^{-6}	-3.78592	-0.8877	
Sintering Temp.=950^{o}C	823	1.21483	280.32175×40^{-6}	-3.56232	-0.6374	
Sintering time= 4hrs.	873	1.14526	503.89603×10^{-6}	-3.29868	-0.3566	
	923	1.08323	1.10925×10^{-3}	-2.95826	+0.0099	
	973	1.02758	1.75268×10^{-3}	-2.7563	+0.2323	
	1023	0.977364	3.42909×10^{-3}	-2.46484	+0.5448	
	1073	0.931827	6.20733×10^{-3}	-2.20711	+0.8235	
	1123	0.890345	11.1244×10^{-3}	-1.95373	+1.0966	
	1153	0.867182	14.97675×10^{-3}	-1.82459	+1.2371	

Table 4.2: A.C. conductivity at different temperatures for compacting pressure 11000 lbs.

History of the Sample	Temp. $T^{\circ}K$	$\frac{1}{T} \times 10^3$ $(^{\circ}K)^{-1}$	Specific conductivity σ $(ohm\text{-}cm)^{-1}$	$\log \sigma$	$\log \sigma T$	Remarks
Sample B	523	1.91146	4.52079×10^{-6}	-5.34478	-2.6264	
	573	1.74471	19.83959×10^{-6}	-4.70247	-1.9446	
Weight = 1.918 gms	623	1.60472	63.56381×10^{-6}	-4.19679	-1.4023	
Length = 0.684 cm	673	1.48553	159.37847×10^{-6}	-3.79756	-0.9697	
Dia. = 1.123 cm	723	1.38281	305.9077×10^{-6}	-3.51441	-0.6523	
Bottom electrode G.Ring Dia =0.893 cm	773	1.29339	561.78988×10^{-6}	-3.25044	-0.3623	
Sintering Temp.=950°C	823	1.21483	1.03662×10^{-3}	-2.98439	-0.0600	
Sintering Time = 4 hrs.	873	1.14526	1.78046×10^{-3}	-2.74946	+0.1924	
	923	1.08323	2.37852×10^{-3}	-2.6247	+0.3414	
	973	1.02758	3.35739×10^{-3}	-2.47396	+0.5140	
	1023	0.977364	6.26757×10^{-3}	-2.20291	+0.8070	
	1073	0.931827	10.92095×10^{-3}	-1.96174	+1.0689	
	1123	0.890345	19.92592×10^{-3}	-1.70058	+1.3497	
	1153	0.867182	27.14977×10^{-3}	-1.56623	+1.4955	

Table 4.2: A.C. conductivity at different temperatures for compacting pressure 13000 lbs.

History of the Sample	Temp. $T^{\circ}K$	$\frac{1}{T}\times10^{3}$ $(^{\circ}K)^{-1}$	Specific conductivity (ohm σ cm)$^{-1}$	$\log\sigma$	$\log\sigma_T$	Remarks
Sample C	505	1.9801	4.78138×10^{-6}	-5.3205	-2.6173	
	562	1.779	23.9684×10^{-6}	-4.6204	-1.8706	
Weight = 1.930 gm	645	1.5504	134.9876×10^{-6}	-3.8699	-1.0602	
Length = 0.667 cm	719	1.3908	388.631×10^{-6}	-3.4105	-0.5538	
Dia. = 1.129 cm	798	1.2531	859.880×10^{-6}	-3.0655	-0.1635	
Bottom electrode ~~G. Ring~~ Dia = 0.893 cm	889	1.1249	2.24965×10^{-6}	-2.6480	+0.3008	
Sintering Temp.=950°C	981	1.0193	6.30576×10^{-3}	-2.2004	+0.7914	
Sintering Time = 4 hrs.	1053	0.9496	13.14762×10^{-3}	-1.8116	+1.1402	
	1104	0.9057	20.72238×10^{-3}	-1.68359	+1.3593	

Table 4.2: A.C. Conductivity at different temperatures for compacting pressure 15000 lbs.

History of the Sample	Temp. ^{o}K	$\frac{1}{T} \times 10^{-3}$ $(^{o}K)^{-1}$	Specific conductivity σ $(ohm-cm)^{-1}$	Log σ	Log σ_T	Remarks
Sample D	505	1.9801	7.23644×10^{-6}	-5.1405	-2.4373	
	582	1.7182	60.098×10^{-6}	-4.22113	-1.4563	
Weight = 1.930 gm	645	1.5504	210.08×10^{-6}	-3.67758	-0.8681	
Length = 0.650 cm	719	1.3908	586.07×10^{-6}	-3.23203	-0.3753	
Dia. = 1.444 cm	798	1.2531	1.4090×10^{-3}	-2.82681	+0.0508	
Bottom electrode Dia. = 0.893cm.	854	1.1709	2.55348×10^{-3}	-2.59296	+0.3385	
Sintering Temp. = 950°C	981	1.0193	9.39×10^{-3}	-2.02733	+0.9643	
Sintering Time = 4 hrs.	1053	0.9496	23.697×10^{-3}	-1.62526	+1.3971	
	1104	0.9057	34.6432×10^{-3}	-1.46052	+1.5826	

Table 4.2: A.C. conductivity at different temperatures for compacting pressure 7000 lbs.

History of the Sample	Temp. (^oK)	$\frac{1}{T}x10^3$ $(^oK)^{-1}$	Specific conductivity σ $(ohm-cm)^{-1}$	Log σ	Remarks
Sample E	523	1.91146	$4.78849x10^{-6}$	-5.31980	
	573	1.74471	$21.03003x10^{-6}$	-4.67717	
Weight = 1.951 gms.	623	1.60472	$67.84910x10^{-6}$	-4.16845	
Length = 0.705 cm	673	1.48553	$168.66455x10^{-6}$	-3.77303	
Dia = 1.105 cm	723	1.38281	$323.61972x10^{-6}$	-3.48994	
Bottom electrode G. Ring Dia = 0.893 cm	773	1.29339	$629.48929x10^{-6}$	-3.20001	
Sintering Temp1=950°C	823	1.21483	$1.24903x10^{-3}$	-2.90344	
Sintering Time = 4 hrs.	873	1.14526	$2.11684x10^{-3}$	-2.67432	
	923	1.08323	$2.47845x10^{-3}$	-2.60581	
	973	1.02758	$4.31431x10^{-3}$	-2.36511	
	1023	0.977364	$7.49929x10^{-3}$	-2.12495	
	1073	0.931827	$11.21285x10^{-3}$	-1.84732	
	1123	0.890345	$25.79507x10^{-3}$	-1.58807	
	1153	0.867182	$40.318558x10^{-3}$	-1.39449	

* These results are not plotted. We are however taking $\sigma_{100°C}$ = 176·1 m℧/cm.

done below 1000°C. Heating to 1000°C ensures the dimensional stability and ~~also equilibrium concentration of defects and~~ proper contact of the electrode plates thereby eliminate the hysteresis.

There is a break in the slope of the curves in the region 600 and 665°C. The curves are resonably straight below and above this range.

It should be noted that the curves obtained in the present study are analogus to that of Ure's result for YF_3 - doped CaF_2 single crystals as shown in the Figure 4.3(b). In Ure's study the break in the slope of the curves was found between 550°C and 650°C and the behaviour was quite different above and below the break. In the lower temperature range the lines were resonably straight but it was not the case in high temperature range (Fig. 4.3b).

In Figure 4.2 the variation of electrical conductivity. With temperature for pure single crystal as obtained by Ure is replotted along with the present work. The figure shows that powder compacts have higher conductivity at all temperatures. This can be explained in terms of the grain boundaries in compacts. The powder compacts are polycrystalline with large grain boundaries areas. It is known that in the region of grain boundaries there exists considerable structural uncertainties and defects. All these may contribute to enhanced mobility of the carge carrier. In otherwords near grain boundaries the diffusion is more than that in the bulk. Thus presense of grain boundaries affect the overall conductivity.

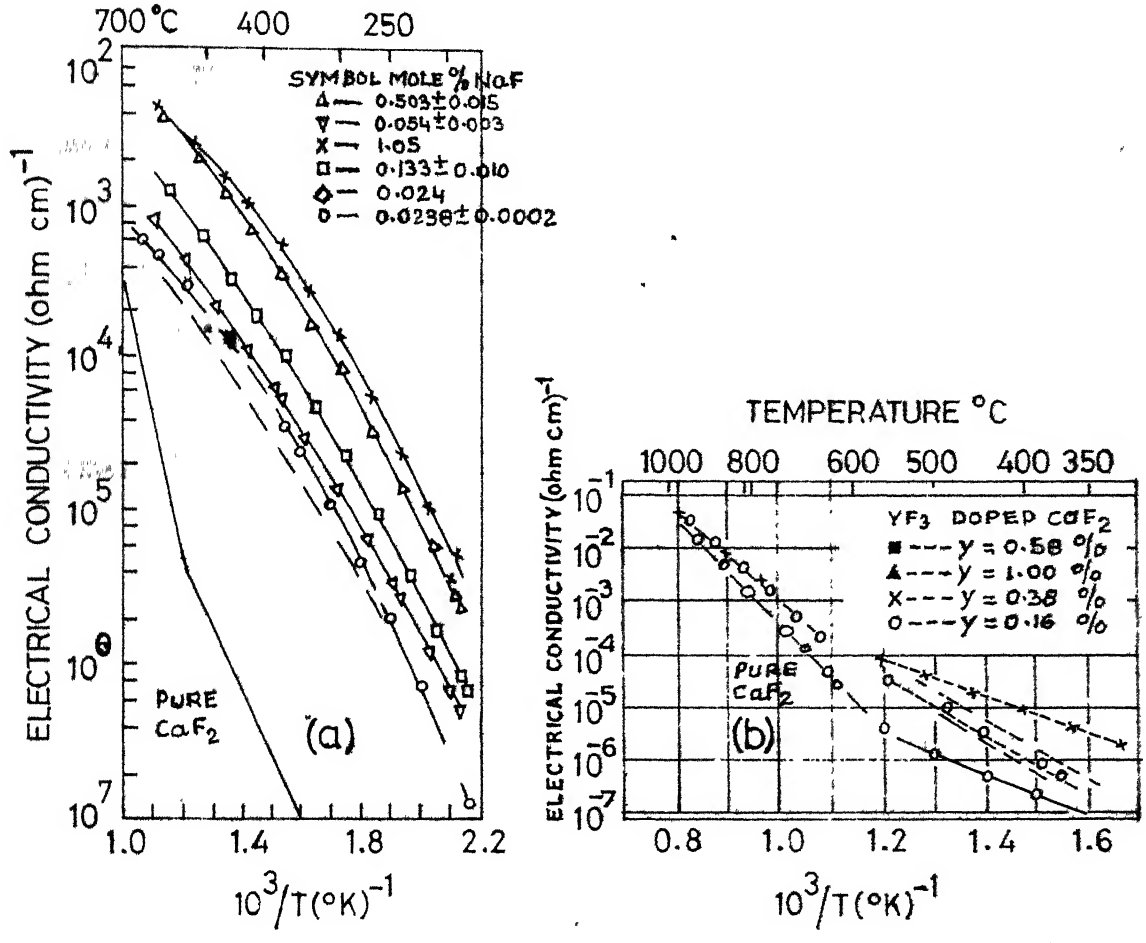

FIG. 4.3 ELECTRICAL CONDUCTIVITY OF CaF_2 CRYSTALS DOPED WITH (a) NaF (b) YF_3

Osburn and Vest[34] in their study on electrical properties of single crystals, bicrystals and polycrystals of MgO found that grain boundaries enhanced ionic conductivity. This was attributed to increased vacancy concentration at grain boundaries leading ~~to decreased activation energy~~ a easier mechanism for the motion.

The data obtained in the present investigation (Fig.4.2) may be compared with the results of Ure (Fig. 4.3) on doped single crystal. In case of YF_3 - doped crystals the conductivity is increased due to introduction of an excess of F^- interstitial along grain boundaries. In the present case the increase is due to the increased defect concentration in the grain boundaries, and a easier mechnism of motoin along the grain boundary.

Figure 4.2 also points out that conductivity of the compacts increases as the compacting pressures increase. This can be explained on the basis of densification. The conductivity values of the specimens could be expected to rise due to contact areas merging and forming more and more continuous matrix.

Figure 4.4 shows a plot of conductivity vs. porosity. It is observed that as the porosity increases the conductivity decreases. This may be attributed to densification of the compacts.

Activation energies have been calculated from the slopes of the log σ vs. 1/T using the least square technique with the help of computer. As shown in the figure 4.2 each curve consists of two straight line portions and indicates two activation energies for the two different temperature ranges. At high temperatures, the thermal energy is sufficiently high to

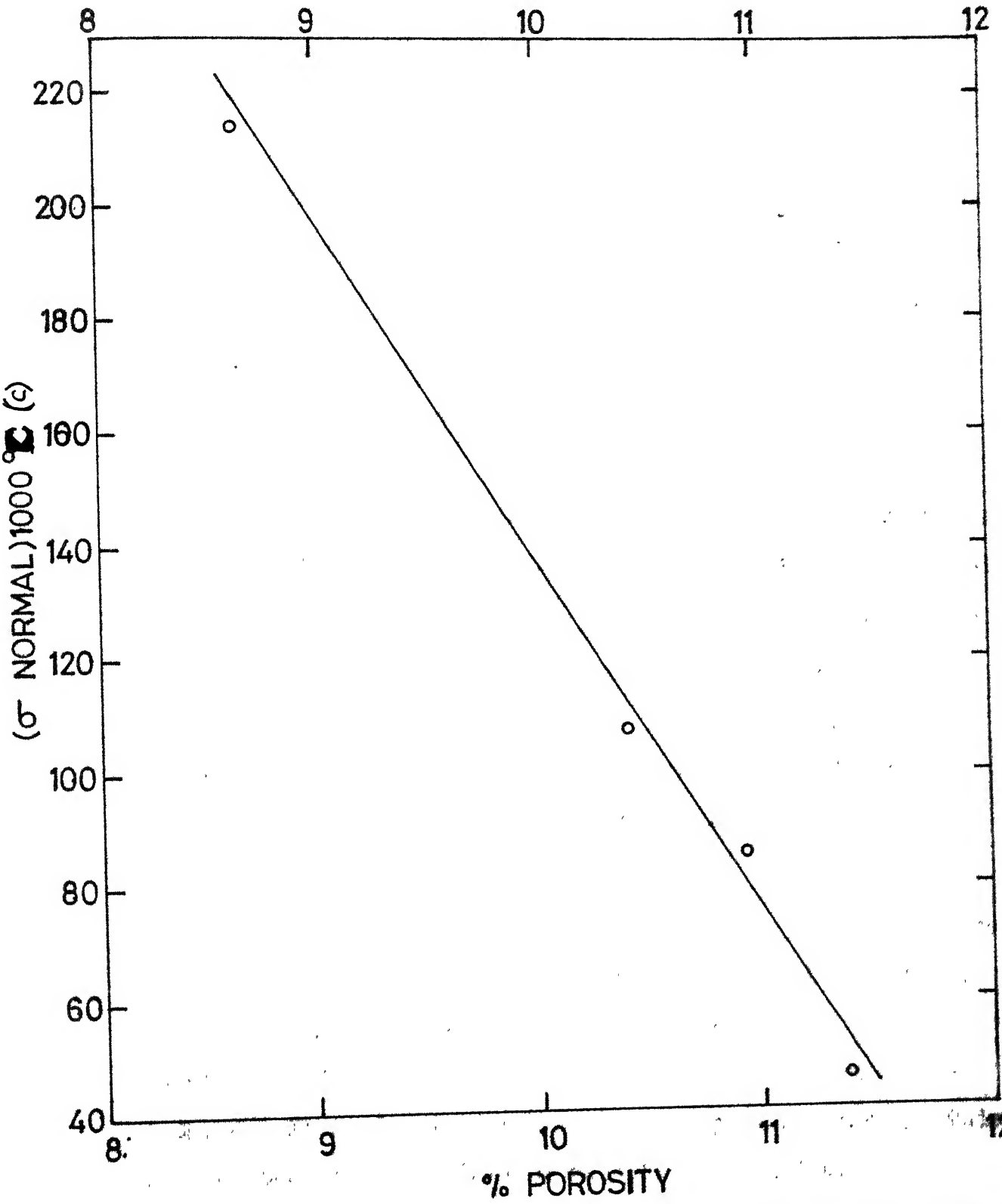

FIG.4.4 CONDUCTIVITY CHANGE OF CaF_2 COMPACTS WITH POROSITY

create defects (vacancies and interstitials $\overline{F}$), and the activation energy is the sum of the energy for the formation of defects and its migration in the bulk. At lower temperatures the thermal energy is only large enough to allow the thermal energy is only large enough to allow the migration of atoms into vacancies already present in the crystal. Table 4.3 shows the activation energy in the extrinsic and intrinsic regions.

4.3 Microstructure Study:

Microphotographs obtained for compacting pressures of 11000 lbs, 13000 lbs and 15000 lbs at magnification 100 X are shown in Figure 4.7 a to c. For the 1st specimen microphotograph at magnification 210 x was also taken and is shown in Fig.4.7d.

Microstructures directly indicate the degree of densification which should be known both for research purposes as well as for commercial applications. Elimination of excessive porosity is necessary. This enhances such properties as elasticity, strength, capacitance, optical transmission and also helps in removal of trapped gases.

From the microphotographs shown in Fig. 4.7 it is evident that as compacting pressure increases the size of the grains becomes larger and larger and pores are eliminated. Microphotographs for 11000 lbs and 13000 lbs compacting pressures are compared. It is found that the latter has less porosity. This confirms the trend obtained by density calculations.

From the negative the A.S.T.M. micrograin size and nominal grains/in^2 were measured and are shown in the table 4.4. As

Table 4.3: Activation energies for different compacting pressures.

Sample	Pressure	Activation energy (Kcal/mole)	
		Extrinsic	Intrinsic
A D	5000	14.290	24.672
B C	11000	14.769	25.577
C B	13000	14.564	20.896
D A	15000	13.760	23.241
* E	7000	15.074	29.971

* Results discarded

146 grains/sq.in in the original negative which was at 10

Fig. 7(c): Microphotograph of CaF_2 compact at compacting pressure 15000 lbs. Magnification, 100 X 4 approx

Fig. 7(d): Microphotograph of CaF_2 compact at compacting pressure 11000 lbs. Magnification, 100 X 4 approx.

Table 4.4: Average number of grains for different compacting pressures.

Microform Reader magnification = 19.56 X
Negative Magnification = 100 X
Total Magnification = 1956 X
Scan Length = 30 cms.

Sample	Compacting pressure	Number of Grains		Av.No. of grains	A.S.T.M. Micro-grain size	Nominal grains/in^2 at 100X
		From one end	From the other end			
E	7000	13 12 10 8 9 14	12 10 13 13 14 13	11.75	9.25	287
B	11000	10 11 10 12	10 11 10 11	10.625	9.0	256
C	13000	6 5 6 5	6 6 5 5	5.5	Between 7.0 to 7.25	64 to 71.7
D	15000	6 6 6 5	6 6 4 4	5.37625	7.0	64

compacting pressure increases the averages number of grains decrease and so do the A.S.T.M. micrograin size and consequently nominal grains /in^2. The reason for less nominal grains/in^2 at higher pressures is due to grain growth since the pores are eliminated.

A plot of A.S.T.M. micrograin size vs.pressure is shown in Figure 4.5. Figure 4.6 shows the variation of electrical conductivity with nominal grains /in^2. Please see Dr. H.S. Ray of Met. Engg. Deptt., for Reference.

The conductivity variations may be explained by the microstructures. During sintering air-gaps are eliminated and the conductivity is enhanced because of decrease in contact resistance. Thereafter, when grain growth occurs, the size and perfection of the grains and the nature of the grain boundary control the conductivity.

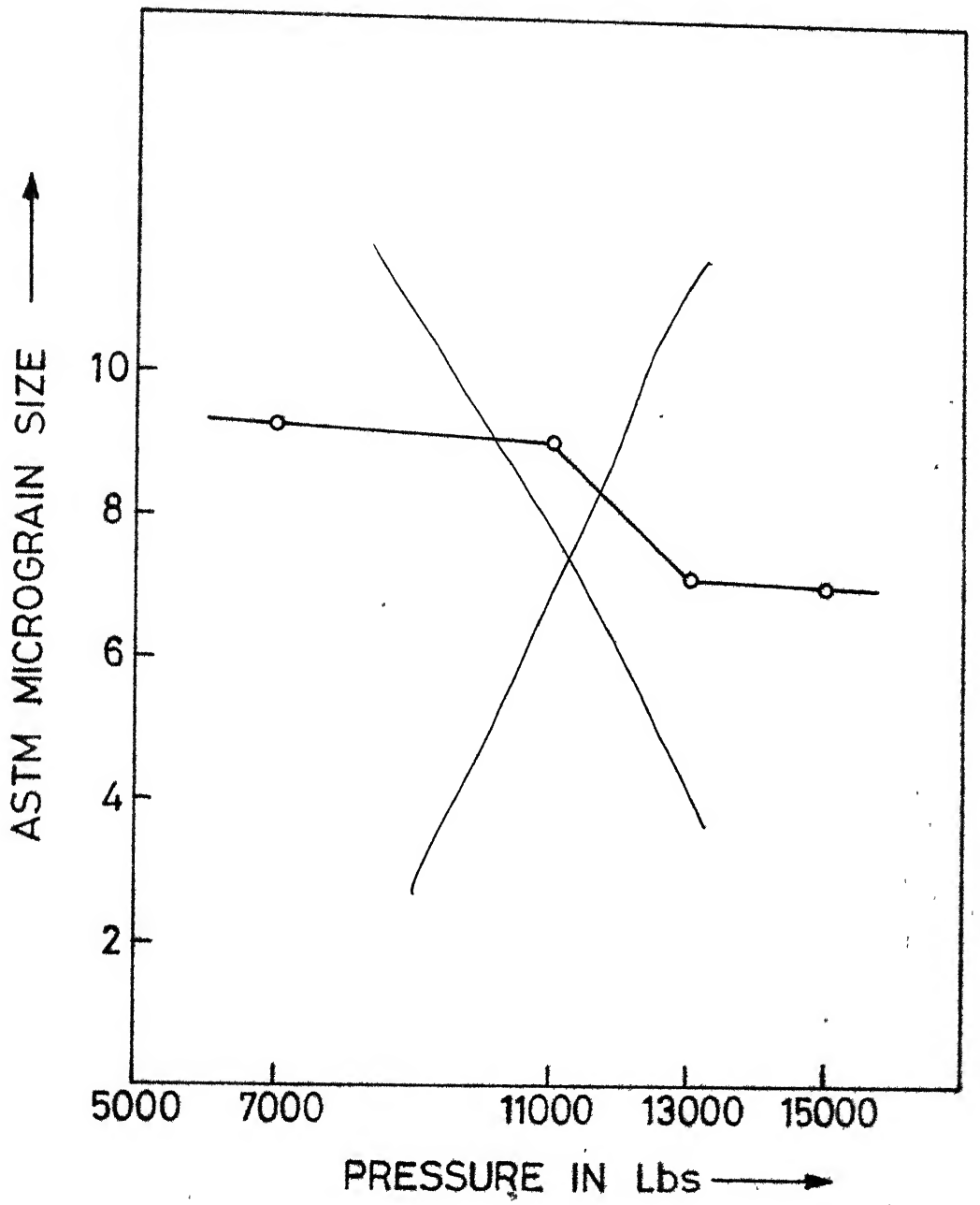

FIG. 4.5 VARIATION OF MICROGRAIN SIZE WITH COMPACTING PRESSURE

* Please see Dr. H.S. Ray of Met. Engg. Deptt., IIT/K for References.

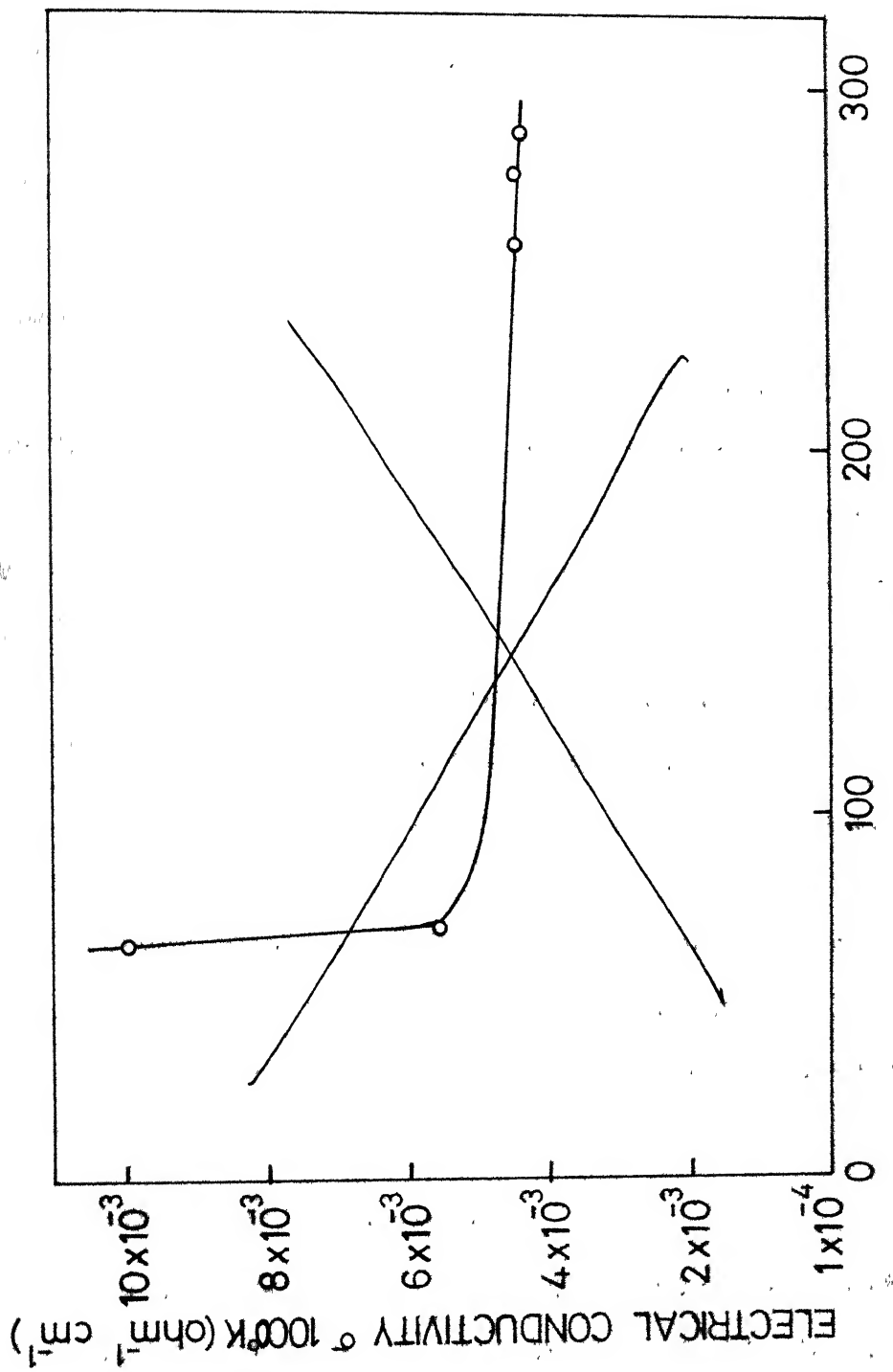

FIG. 4.6 CONDUCTIVITY VARIATION WITH NOMINAL GRAINS/IN^2

* Please see Dr. H.S.Ray of Met. Engg. Deptt., IIT/K for reference.

CHAPTER V

CONCLUSIONS

The main conclusions of the present investigation are as follows:

1. Denser green compacts produce denser material after sintering.
2. A slightly higher sintering temperature than 950°C is needed for getting a more dense product.
3. Electrical conductivity for powder compacts is higher than that of single crystal at all temperatures.
4. Electrical conductivity of the powder compact depends upon the porosity. If the porosity is higher, the conductivity is lower and vice-versa.
5. A.S.T.M. micrograin size and nominal grains/in 2 decrease with the increase of the compacting pressure.
6. Electrical conductivity decreases as the nominal grains/in^2 increase.
7. Powder compacts of CaF_2 may be used in physico-chemical measurements as a fluorine ion conducting solid electrolyte. These would be useful for liquid systems also as crucibles may be fabricated from powder compacts.

Suggestions for Future Work:

Due to lack of time the present study was restricted to samples compacted under various pressures but all sintered at the same temperature for equal length of time. The study could be extended to systematically investigate the effect of sintering time and temperature.

For better understanding of the phenomenon of conductance the measurement of frequency dependence of conductivity is recommended. This could not be done in the present investigation due to lack of suitable equipment. However, this should be taken up in future.

The effect of grain boundaries on conductance can be critically revealed by measurement on a bicrystal where the grain boundary is very well defined. A suitable bicrystal may be grown for this purpose and its conductivity measured in a direction parallel to the grain boundary and also in one perpendicular to it.

The present work does not reveal the dependence of conductivity on particle size. This would be somewhat irrelevent unless the porosity is controlled. It would be interesting to start with various particle sizes and conductivities may be compared with identical porosity.

Finally the study indicates that CaF_2 powder compacts may be used in physico-chemical experiments as a fluorine ion conductor. This may be substantiated by direct measurements of e.m.f. also employing powder compacts as solid electrolyte. Since powder compacts may be made in the form of crucibles, measurements involving liquids may also be done using such crucibles.

REFERENCES

1. K. Kiukkola and C. Wagner, J. Electrochemical Soc. 1957, 104, p. 379.

2. R.T. Foley, J. Electrochemical Soc. Jan. 1969,0.13 C.

3. R.W. Ure, Jr, The J. of Chem. Physics Vol. 26, No. 6, 1957, p. 1363.

4. A. Robert Rapp, A David Shores, 'Solid Electrolyte Galvanic Cells in Techniques of Metals Researeh' Ed. R.F. Bunshah, Vol. 4, Part 2, 1970 p. 123.

5. M.F. Berard, J. Am. Cera Soc. Marcb 1971, p. 145.

6. R.C. Evans, In Introduction to Crystal Chemistry, Cambridge at the University Press, 1964, p. 147.

7. Hansjoachim Matzke, J. Nucl. Mater. 11|3|, 1964,p. 344.

8. R. Baker and J.M. West, J. Iron and Steel Inst. 204 1966, p. 212.

9. James Short and Rustum Roy, J. Phy. Chemistry, Vol. 67, Sept. 1963, p. 1860.

10. E. Barris and A. Taylor, J. Chem. Physics,(45),1966, p. 1154.

11. T.L. Markin,Symposium on E.M.F. Measurements in High Temperature Systems, Inst. Min. Met (London) Ed. C.B. Alcock, 1968, p. 90.

12. N.L. Lofgren and E.J. McIver, U.K. A.E.A, A.E.R.E, R 5169, 1966, 17 p.

13. R.J. Bones, T.L. Markin and V.J. Wheeler, Proc. Brit. Ceramic Soc. 1967, 8, p. 51.

14. J.J. Egan and R.J. Hens, J. Phys. Chem. 49, 1966, p.38.

15. D. V. Vecher and A.A. Vecher, Zh, Fiz, Khim, 1967, 41, p. 2916.

16. R. Benz and C. Wagner, J. Phys. Chem. 1961, 65, p. 1368.

17. T.N. Rezukhina, Leisskii and M. Ya. Frenkel Izv. Akad, Nauk, U.S.S.R. Neorgan Matinaly, 1966, 2, p. 325.

18. T.N. Rezukhina and Ya. Baginska, Electrochimiva, 1967, 3,p. 114.

19. K.K. Prasad and K.P. Abraham, Proc. of Symp. on Mat. Sc. BARC-NAL Bangalore 1969.

20. K.K. Prasad and K.P. Abraham (Unpublished work).

21. S. Ragavan and K.P. Abraham (Unpublished work).

22. S. Aronson, J. Inorg. Nucl. Chem. 1967, 29, p. 1611.

23. K.A. Gingerich and S.Aronson, J. Phys. Chem. 1966, 70, p. 2517.

24. S. Aronson and J. Sadofsky, J. Inorg. Nucl. Chem. 1965, 27, p. 1769.

25. S. Aronson, Int. Conf. Compounds of Interest in Nuclear Reactor Technology (Boulder, Colo, AIME) 1964, Vol. 10, p. 376.

26. W.K. Behl and J.J. Egan, J. Electrochem. Soc. 1966, 113, p. 376.

28. S. Aronson and A. Auskern, Thermodynamics (Vienna, IAEA) 1965, Vol. 1, p. 165.

28. F. Moattar and J.J. Anderson, Trans. Faraday Soc. 1971, 67, p. 2303.

29. L. Heyne, Electrochimica Acta, 1970, Vol. 15, p.1251.

30. Williana C. Coones, Ceramic Microstructures their analysis, significance and production, proc. of the 3rd. Int. Materials Symp. held at Berkeley 1966, p. 187.

31. E.B. Allison and P. Murray, Acta, Metallurgica, Vol. 2, 1954, p. 487.

32. H.C. Graham, N.M. Tallan and Ralston Russell Jr., J.Am. Ceram.Soc. Vol. 50, 1967, p. 156.

33. F.S. Bragner and R.N. Blumenthal, J. Am. Ceram. Soc. March 1971,

34. C.M. Osburn and R.W. Vest, J. Am. Ceram. Soc. Vol. 54, No. 9, 1971, p. 428.